The 8th International Conference on Jets, Wakes and Separated Flows, ICJWSF-2024
September 23-25, 2024, Firenze, Italy

Feasibility Study on Development of Return Guide Vane Using Jet Flow for Compact Multi-Stage Centrifugal Compressors

T. Fujii[1] *, M. Koga[1] , M. Kudo[1] , K. Nishibe[1] and K. Sato[2]

[1] Graduate School of Integrative Science and Engineering, Tokyo City University, Japan
[2] Department of Mechanical System Engineering, Kogakuin University, Japan

* Correspondent author: g2381052@tcu.ac.jp

Abstract

This study examined the feasibility of miniaturizing and simplifying return guide vanes (RVs) using jet flow as a first step in developing compact multi-stage centrifugal compressors for cooling high-density optical and medical equipment. We adopted a cylinder as an example of the simplest vane inside the return channel with a large ratio of inside and outside compressor diameters. We investigated the effects of RVs on the internal flow, flow loss, and the residual swirl component via experiments and numerical simulations. The results confirmed that the proposed RV is effectively suppressed the flow instability generated in the swirling flow, and that stable operation can be realized. In addition, the total pressure drop and residual angular momentum of the proposed RV were lower at the device outlet than for conventional RVs under the same conditions, demonstrating improved efficiency.

Keyword: *Return guide vane, Swirling flow, Active flow control, Flow instability, Coanda effect*

1. Introduction

Multi-stage centrifugal compressors used for pressurizing working fluids in power plants and energy plants are used under long hours of continuous operation, so high efficiency and stability are essential. Numerous studies have been conducted to optimize the geometry of diffusers, return channels, and return guide vanes in addition to impellers as the rotating parts, using inverse problem analysis methods and multi-objective optimization [1-3]. As a result, improvements of internal flow and performance, mainly at the design flow rates and pressures, have been confirmed. The application of jetting technology has been begun to suppress flow instability and improve performance degradation that occurs under operating conditions other than the design flow rates and pressures [4-5]. Ohtani reported that the swirl stall that occurs at low flow rates had been suppressed and the stable operating range had been expanded by injecting jet flow from near the leading edge of a circular vane row that looks like the rotor vanes of a centrifugal compressor [4]. Our research group is also developing a slotted return guide vanes (hereinafter referred to as "slotted RV") [5] to improve the efficiency of the return channel and RV systems [6], which has been reported to cause a 5% to 10% drop in the overall efficiency of multi-stage centrifugal compressors. The development of slotted RVs [5] is underway to improve the efficiency of return channel and RV systems [6]. When the flow rate (flow angle) deviates from the design values, the large-scale separation generated by the secondary flow between the RVs was one of the causes of the efficiency loss mentioned above. Therefore, we attempted to improve the flow between RVs by supplying the jet flow to the suction surface of the RV. As a result, the flow field has been improved, and flow resistance and residual angular momentum have been reduced successfully by injecting the jet flow which is approximately 3% of the operating flow rate. In recent years, optical and medical equipment and energy recovery systems have been miniaturized, and the internal components of such equipment have become denser. Therefore, it is difficult for conventional axial flow fans to provide sufficient air cooling for the heating elements in the above-mentioned equipment and systems, so compact multi-stage centrifugal compressors which can realize high differential pressure seem to be used. Thus, it is expected that RV with the jet flow described above will be applied to small multi-stage centrifugal compressors to improve their efficiency. However, since this technology is based on Coanda effect of the suction surface of the RV, it is unclear whether

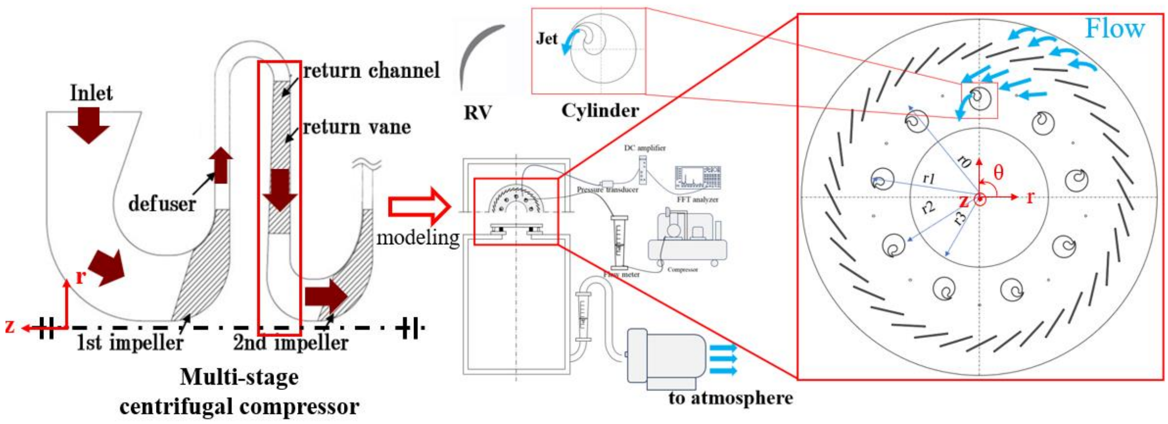

Fig.1 Experimental apparatus

Table 1. Numerical analysis

	3D analysis	2D analysis
CFD code	Ansys CFX 2022R1	
Assumption	3D incompressible viscous flow	2D incompressible viscous flow
Operational fluid	air	
Analysis type	Steady state	Unsteady state
Governing equation	RANS	URANS
Turbulence model	k- ω SST	
Mesh shape	Tetra	
Mesh number	3,000,000	200,000
$y+$ (near RV)	< 1	
Wall function	Automatic	

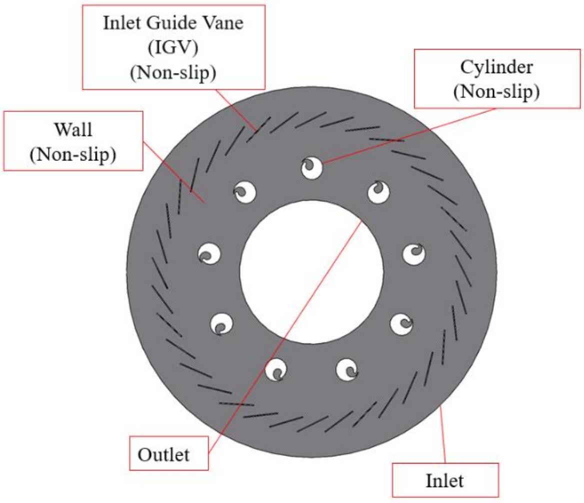

Fig.2 Analysis model

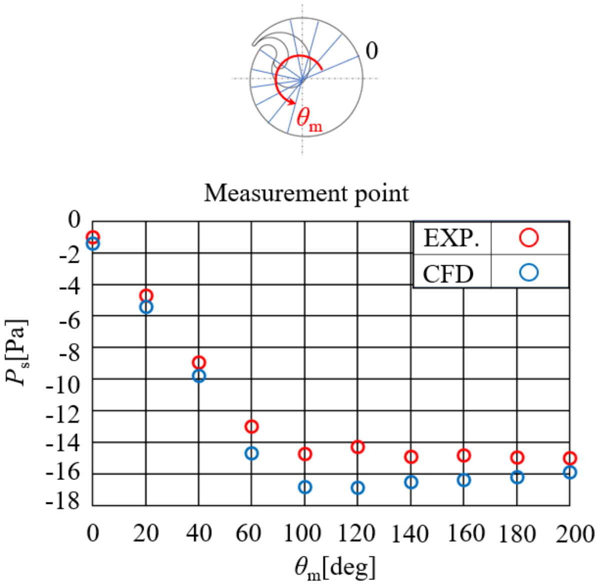

Fig.3 Measurement point and validation

this technology will be useful in environments where sufficient curvature and the number of vanes cannot be maintained due to downsizing.

In this study, as a first step in verifying the applicability of slotted RVs using jets to the compact multi-stage centrifugal compressor, a cylinder was adopted as an example of the simplest basic shape of a vane inside a return channel with a large ratio of inside and outside diameters of the compressor, and its effect on the internal flow, pressure recovery performance, and the suppression of circumferential velocity at the equipment outlet were investigated from both through model experiments and numerical simulations. This paper examines whether the proposed slotted RVs can suppress the unstable flow [7-8] that has been reported to occur in an inward swirling flow. The differences in performance (residual total pressure and residual angular momentum) between conventional RVs and the proposed slotted RVs in a swirling flow with an inlet guide vane installation angle γ = 20° have been discussed.

2. Experimental Apparatus and Method

Fig.1 shows an overview of the multi-stage centrifugal compressor and a schematic diagram of the experimental apparatus when equipped with slotted RVs. The vane shapes of the test channel and conventional RVs are based on the research by Kanemoto et al. [3] on circular vane rows for the return channel of centrifugal turbomachinery. Therefore, this experiment does not consider the velocity distribution deviation from the hub to the shroud side in the return channel, which is confirmed in the actual machine when the flow is diverted. Inward swirling flow is generated downstream of 36 inlet guide vanes (IGVs) (chord length 30 mm, blade thickness 1 mm, blade width 10 mm, installation angle γ = 20°) installed at r = 125 mm by suction from a plenum tank connected to the channel between the two plates using a blower. The leading edge of a conventional RV (L.E. installation angle α_1 = 24.8°, T.E. installation angle α_2 = 90°, 10mm blade width, 9 blades) was installed downstream of the IGV at r = 90 mm, and the proposed slotted RV was installed so that the center of the cylinder (slot installation angle θ = 44°, slot height 1 mm, diameter 20 mm, span 10 mm, 9 slots) was located at the same radius. High-pressure air generated by a compressor with adjustable pressure inside the cylinder was supplied to the cavity (6 mm in diameter and tapered down in the span direction) from one side of the cylinder through an area-type flow meter to adjust the jet flow rate from the slot. Ten static pressure measurement holes (0.3 mm in diameter) were provided circumferentially in the center of the span of the slotted RV. The wall static pressure P_s, which is the pressure difference between the atmospheric pressure and the static pressure on the suction surface of the vanes, was measured by connecting a pressure transducer. Measurements of pressure fluctuation waveforms and phases due to flow instability were performed using an FFT analyzer.

3. Computational Fluid Dynamics Setup

Table 1 and Fig.2 show the CFD analysis conditions, analytical model, and boundary conditions, respectively. The flow instability generated in an inward swirling flow was verified by unsteady analysis (governing equations: Unsteady-Reynolds-Averaged Naiver-Storks (URANS), total number of meshes: approximately 200,000) A three-dimensional steady-state analysis (governing equations: RANS; total number of meshes: approximately 3 million) was conducted to investigate the suppression effects of total pressure loss and residual circumferential velocity components using conventional and slotted RVs, assuming a generally steady flow is generated. For both analyses, the k-ω SST model and Automatic [9] (automatic near-wall treatment automatically switches from wall-functions to a low-*Re* near wall formulation as the mesh is refined) were adopted for the turbulence model and wall function, respectively. They were set so that $y+ < 1$ near the vane. The inlet and outlet surfaces of the analytical domain were specified with a total pressure assuming an atmospheric release, and constant mass flow rate G, respectively. The jet flow rate from the slot outlet of the proposed slotted RV was specified by the mass flow rate G_s, and the no-slip condition was applied to each wall surface. The steady-state criterion was defined as RMS values of velocity, pressure, and turbulence energy less than 1.0×10^{-4}. The Simple pressure solution method was used, and the advection term was discretized by a high Resolution [9] (a combination of first- and second-order upwind difference approximation). Fig.3 shows the time-averaged wall static pressure distribution for a slotted RV without blowing (G_s = 0kg/s) obtained from experiment and CFD analysis. The figure shows that the experimental and CFD values correspond qualitatively. The flow increased along the wall in the region of gradually decreasing pressure drop at $0° \leq \theta \leq 100°$, and the flow separated from the wall in the range of approximately constant pressure at $\theta > 100°$ from the velocity fields of the CFD results.

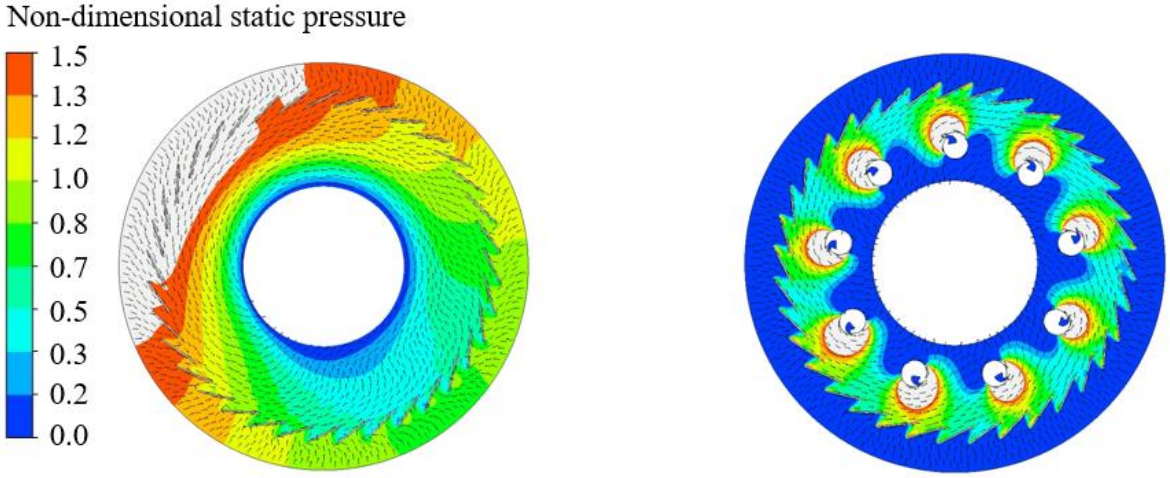

(i) Without RV **(ii) Proposed slotted RV**

Fig.4 Effect of jet flow on flow instability

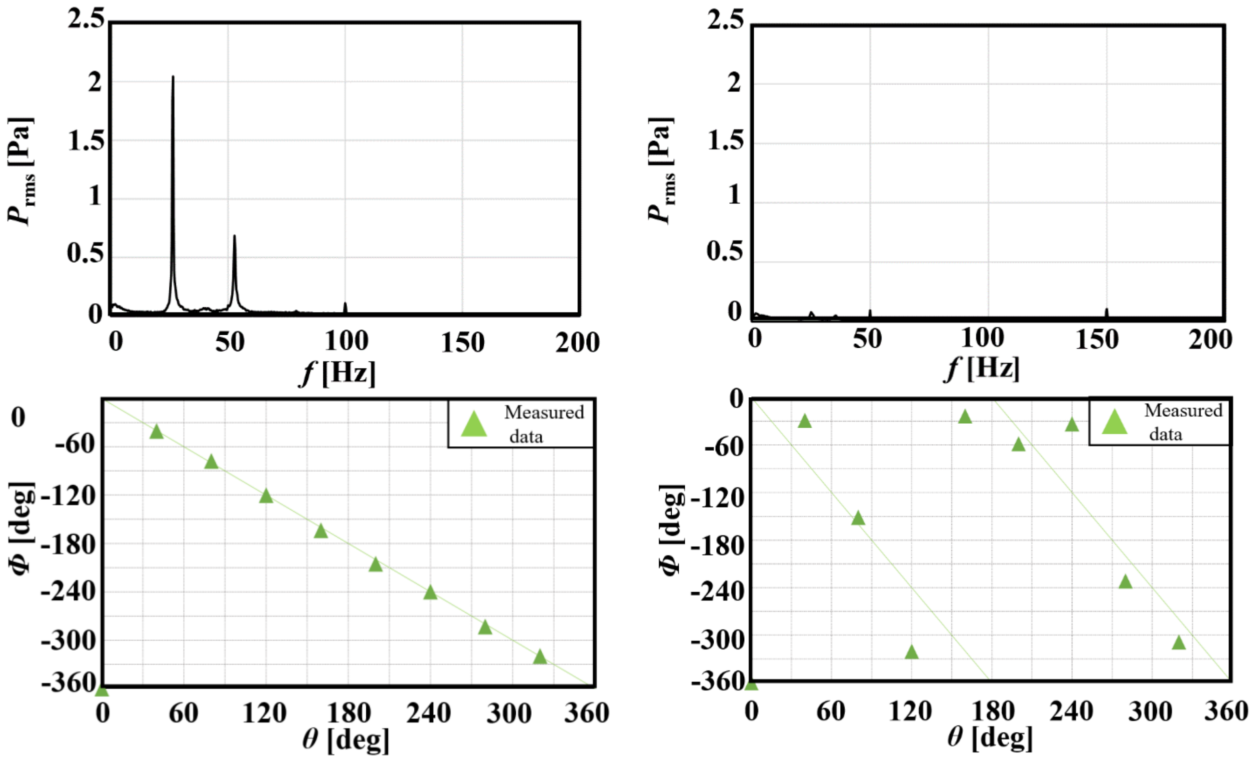

(i) Without RV (1cell) **(ii) Proposed slotted RV (2cell)**

Fig. 5 Power spectrum and phase differnence (Lines express theoretical values)

4. Results and Discussion

4.1 Influence of jet flow on flow instability in inward-swirling flow

Fig. 4 shows the instantaneous normalized velocity vector and dimensionless static pressure coefficient P_s^* (= P_s /P_{sr0}) obtained from a two-dimensional analytical unsteady analysis under the conditions of γ = 20° and the inlet flow velocity specification V = 1.1 m/s. Fig. 5 shows the results of the frequency analysis of the pressure fluctuations on the disk wall (a) and the fluctuation phase (b) obtained from the experiment conducted under the same conditions. Panel (i) simulates the vanless case (no RV), and panel (ii) simulates the slotted RV (corresponding to G_s /G = 0.1).

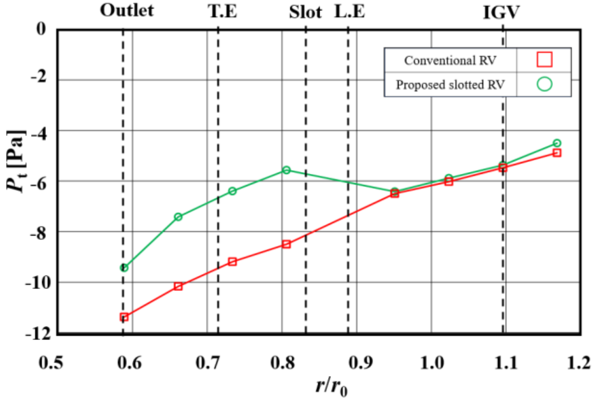

Fig. 6 Total pressure distribution

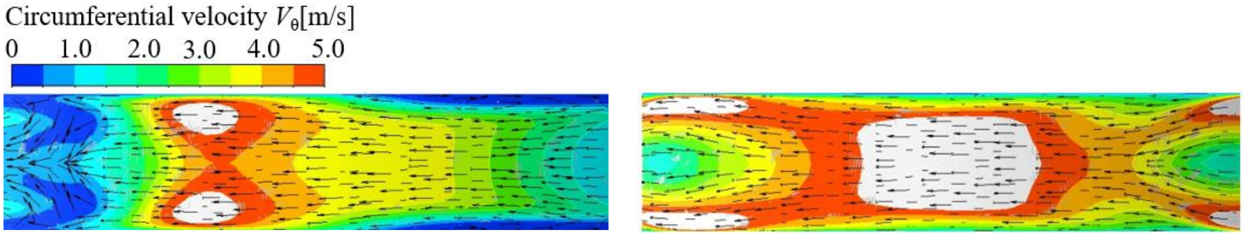

(i) Conventional RV (ii) Proposed slotted RV

Fig. 7 Normalized velocity vector and circumferential velocity distribution at the device outlet

In Fig. 4(i), the white high-pressure and blue low-pressure areas exist as a pair (hereafter referred to as "cells"). The flow propagates circumferentially in a counterclockwise direction from CFD results at other times, which corresponds well with the outstanding frequency measurement in Fig. 5(i)(a) and the phase difference in Fig. 5(i)(b) obtained from the experiment under the same conditions and indicates that a flow instability with cell 1 is occurring. On the other hand, in Fig. 4 (ii), the velocity vector and static pressure distribution are isotropic, and circumferential velocity decreases near the outlet of the device. In the experimental results shown in Fig. 5(ii)(a) and (ii)(b), no outstanding frequency component or phase difference is observed, as in Fig. 5(i)(a) and (i)(b), indicating a stable flow. Furthermore, the conventional RV also suppresses the flow instability, as in (ii) slotted RV from the same CFD and experimental results. From the above, the proposed slotted RV can suppress a flow instability with pressure fluctuation similarly to the conventional RV, and it can achieve stable operation even at flow angles shallower than the RV installation angle.

4.2 Performance of slotted return guide vane

Fig. 6 shows the total pressure P_t distribution with a transition of r/r_0 obtained from a 3D steady-state analysis at $\gamma = 20°$ and mass flow $G = 0.0069$ kg/s. The square plot shows the conventional RV, and the circle plot shows the slotted RV ($G_s / G = 0.1$). Both conventional and slotted RVs show a decreasing trend in the total pressure toward the device outlet. Comparing the results, the slotted RV was observed to have a larger residual total pressure than that of the conventional RV, owing to the increase of dynamic pressure caused by the added jet flow and maintaining or increasing the total pressure immediately after the slot outlet, resulting in a larger residual total pressure near the outlet than the conventional type. The improved flow field near the RV is also expected to contribute to this effect. However, since the energy recovered is slightly lower than the energy input of the jet, more systematic investigation is needed to determine the optimal angle and position of the slot installation that can reduce the energy input.

Fig. 7 shows the normalized vector and circumferential velocity contour in the $\theta - z$ projection of the device outlet obtained from a 3D steady-state analysis under the same conditions as Fig. 6. For reference, the dimensionless flow-averaged angular momentum lout at the outlet of the device was defined and calculated as follows:

$$l_{out}=\int\frac{\int r\rho v_r(-v_r)v_\theta\, dA}{\int(-v_r)dA} \tag{1}$$

where A is the cross-sectional area. The ratio of l_{out} of the slotted RV to that of the conventional RV is $l_{\mathrm{out}}^* = l_{\mathrm{outP}} / l_{\mathrm{outC}}$. The conventional RV (Panel (i)) has a larger circumferential velocity in a larger area than the slotted RV (Panel (ii)), and the flow is uniform in the spanwise direction. Conversely, the slotted RV (Panel (ii)) with the jet flow shows a partial area of high circumferential velocity; however, the overall circumferential velocity is less than that of the conventional RV. The flow-averaged non-dimensional residual angular momentum was $l_{\mathrm{out}}^* \approx 0.9$. Therefore, introducing the slotted RV in this condition range reduces the total pressure loss and residual angular momentum more than the conventional RV from the CFD results. Therefore, the energy increase in energy generated by the next-stage rotor blade downstream of the RV may improve the operating efficiency of the entire system.

6. Conclusion

This study proposes a cylindrical slotted return vane as a new return guide vane for small multistage centrifugal compressors and compares it with a conventional return vane under constant conditions of γ = 20° and mass flow rate G = 0.0069 kg/s (inlet flow velocity V= 1.1 m/s) to determine whether it can effectively suppress the unstably flow that could occur in an inward swirl flow. The results were compared with those of a conventional return vane in terms of total pressure drop and residual angular momentum at the device outlet. The experiments and CFD results confirmed that slotted RV is as effective as the conventional RV in suppressing unstable flow with pressure fluctuation. The analytical results also showed that under the study conditions, the slotted RV has a larger residual total pressure than the conventional RV and can suppress the residual angular momentum. Therefore, the slotted RV may contribute to improving the operating efficiency of the entire system; however further investigation is required to determine the difference between the input and recovered energy of the added jet flow.

Acknowledgments

The authors would like to thank the Japan Institute of Energy for financial support for this presentation.

References

[1] Otani K., "Effect of Fluid Injection to a Leading Edge of a Circular Cascade on Centrifugal Compressor Performance," Turbomachinery, Vol, 45(6), (2017), p. 358-364, DOI: 10.11458/tsj.45.6_358

[2] Sugiyama C., Fujii T., Nishibe K., Kang D., and Sato K., "Investigation of Internal Flow near Return Guide Vane Using Jet and Suction Flow," Proceedings of the 9th World Congress on Mechanical, Chemical, and Material Engineering, 2023, DOI: 10.11159/htff23.177.

[3] Kanemoto T., and Toyokura T., 1986. "Studies on Circular Cascades for Return Channels of Centrifugal Turbomachinery (2nd Report, Flows and Performance of Cascade)", Bulletin of Japan Society of Mechanical Engineers, Vol. 29, No. 255-23, pp. 2893–2900. DOI: 10.1299/kikaib.52.59.

[4] Veress A., and Van Den B., R., 2004, "Inverse Design and Optimization of a Return Channel for a Multistage Centrifugal Compressor ", ASME Journal of Fluids Engineering, 126(5), pp. 799-806. doi: 10.1115/1.1792258.

[5] Nishida Y., Kobayashi H., Nishida H., Sugimura K., 2012, "Performance Improvement of Return Channel in Multistage Centrifugal Compressor Using Multi-Objective Optimization", ASME Turbo Expo 2012: Turbine Technical Conference and Exposition, GT2012-68671, pp. 685-692. DOI: 10.1115/GT2012-68671.

[6] Rube C., Rossbach T., Wedeking M., Grates D. R., and Jeschke P., "Experimental and Numerical Investigation of the Flow Inside the Return Channel of a Centrifugal Process Compressor," ASME. J. Turbomach, vol. 138, no. 10, pp. 101006, 2016, DOI: 10.1115/1.4032905

[7] Kang D., Shinohara T., Nakamura S., Nishibe K., Sato K., Yokota K., and Ohue H., "Performance degradation and flow instability of axial-flow fan due to upstream obstacle," J. of Fluids Eng. vol. 142, 2020, no. 9, pp. 091207.

[8] Nishibe K., Sato K., Tsujimoto Y., and Yoshiki H., " Control of Flow Instabilities Downstream of Radial Inlet Guide Vanes," J. Fluid Sci. Technol. 6(4), 2011, pp. 651-661.10.1299/jfst.6.651

[9] ANSYS, Inc., "CFX2022 R1 CFX-Solver Modeling Guide" ANSYS, Inc., 2022